A novel data-driven tighten-constraint method for wind-hydro hybrid power system to improve day-ahead plan performance in real-time operation

Chunyang Lai[a,*], Behzad Kazemtabrizi[a]

[a]Department of Engineering, Durham University, Durham, DH1 3LE, UK

ARTICLE INFO

Keywords:
Wind-hydro hybrid power system
Day-ahead plan improvement
Real-time operation
Reliability evaluation
Bilevel model
Game theory

ABSTRACT

Complementary operation has been proven an effective way to handle the increasing levels of renewable energy sources (RESs) integration into the grid. However, due to the relative higher levels of forecast uncertainty associated with RESs outputs, when the hybrid power system operates according to the day-ahead plan in real-time operation, the performance of the system may deviate significantly from the initial expectation in the day-ahead plan. Few research works gauge the effectiveness of the day-ahead plan from the perspective of real-time operation, which inadvertently makes this problem under explored. To handle this problem, in this study, using the wind-hydro hybrid power system (WHHPS) as an example, a novel tighten-constraint method is proposed to guarantee the effectiveness of the day-ahead plan in real-time operation. First, the conventional day-ahead planning model and the real-time operation model are proposed to guide the operation of the WHHPS. Second, considering the lack of connection between day-ahead planning and real-time operation in current research, a novel metric, i.e. *Reliability*, denoted by $\mathbb{R}$, is proposed to evaluate the performance of the day-ahead plan from the perspective of real-time operation given inherent prediction errors of wind power. Third, a data-driven tighten-constraint method is proposed by introducing an adjustment parameter, denoted by λ, to improve the reliability of the day-ahead plan and eventually guarantee the effectiveness of the day-ahead plan from the perspective of real-time operation. Finally, a bilevel Stackelberg model is proposed and reformulated to calculate the adjustment parameter and the whole procedure of using the proposed method is clarified. The effectiveness of the proposed method is tested and verified through a series of case studies at the end of this paper. The results show that (1) the proposed method can improve the reliability of the day-ahead plan under different reservoir status; (2) the proposed method can guarantee a high reliability level of the day-ahead plan without adding any additional computation burden; (3) improving the prediction precision of the adjustment parameter can enhance the efficiency of resource utilization for power generation; (4) over time, the increase in available historical data can enhance prediction accuracy of adjustment parameter and improve the effectiveness of the proposed method even further.

Nomenclature

Abbreviations and Indices

RESs	Renewable Energy Sources.
WHHPS	Wind-Hydro Hybrid Power System.
MILP	Mixed-Integer Linear Programming.
LP	Linear Programming.
MIP	Mixed-Integer Programming.
SO	System Operator.
KKT	Karush-Kuhn-Tucker.
$(\cdot)^d$	Variables and parameters corresponding to day-ahead planning.
$(\cdot)^r$	Variables and parameters corresponding to real-time operation.
t	Index of time periods.

Sets

τ	Set of time.
$B(t)$	Set of periods after period t.

Parameters

Δt	Duration of each time period.
e_N	Conversion factor for generation.
N_w^{min}, N_w^{max}	Minimum and maximum output limits of wind power.
N_h^{min}, N_h^{max}	Minimum and maximum output limits of hydropower.
$Q_{in,t}$	Inflow in period t.
$Q_{o,t}^{min}, Q_{o,t}^{max}$	Minimum and maximum outflow limits of hydropower in period t.

*Corresponding author.
Chunyang.Lai@durham.ac.uk (C. Lai);
behzad.kazemtabrizi@durham.ac.uk (B. Kazemtabrizi)
ORCID(s): 0000-0003-0916-4063 (B. Kazemtabrizi)

$Z_{u,t}^{min}, Z_{u,t}^{max}$ Minimum and maximum reservoir water level limits of hydropower in period t.

Z_u^{ini}, Z_u^{fin} Initial and final reservoir water level limits.

$Q_g^{\min}, Q_g^{\max}$ Minimum and maximum possible generation flow.

$h^{\min}, h^{\max}$ Minimum and maximum possible hydraulic head.

Variables

N_t	Total output of WHHPS in period t.
$\bar{N}$	Average output of WHHPS.
$N_{h,t}$	Hydropower output in period t.
$N_{w,t}$	Wind power output in period t.
$Q_{g,t}$	Hydropower generation flow in period t.
h_t	Hydropower hydraulic head in period t.
$Z_{u,t}$	Reservoir water level at time t.
$Z_{d,t}$	Tailwater level in period t.
$h_{l,t}$	Head loss in period t.
$Q_{o,t}$	Hydropower outflow in period t.
V_t	Reservoir volume in period t.
λ_t	Proposed adjustment parameter in period t.
$y_{r,t}$	Unfulfilled status of the plan in period t.

1. Introduction

1.1. Background

Maximising integration of RESs is an effective way for decarbonising energy systems in an effort to mitigate the negative impacts of green gas emissions and to stem the global energy crisis around the world [1][2]. However, the inherent variability of RESs introduces new challenges for the System Operator (SO) in real-time operation. To mitigate the intermittent and fluctuating nature of wind power, complementary management using reliable and dispatchable energy sources has been proven effective, and the operation optimization of such hybrid power systems has been discussed widely. Depending on the planning time scale, the operation planning of the hybrid power systems can be sorted as long-term operation and short-term operation planning problems. Within the remit of short-term operation planning problems, the day-ahead planning of hybrid power systems has been widely discussed for its practical value in guiding the real-time operation. Within a hybrid power system, the day-ahead plan is usually made in the day before the realisation of the actual real-time operation, and therefore, it is determined based on the forecast results of the resources used in the hybrid power system. Depending on the mix of energy resources used, there can be different types of hybrid power systems. Hydropower[3], thermal[4], hydrogen[5], biomass[6], etc are normally mostly chosen complementary power sources in this context. Considering the advantages of hydropower in terms of flexibility, strong regulation properties [7][8] and its ability in stabilizing price volatility caused by wind power in electricity power markets[9][10], in this paper, we choose wind-hydro hybrid power system (WHHPS) as an example to showcase our method. However, it should be noted that the wind power represents RES whose output contains inherent variability, whereas the hydropower represents the complementary power source[11] whose output can be adjusted according to the RES output fluctuation. Therefore, the method proposed in this paper can be applied to any hybrid power system which consists of a variable RES complemented by a complementary power source.

1.2. Literature review

Any day-ahead planning framework for a WHHPS is predicated on the forecast of the wind power prediction. A lot of research has been devoted to improving the forecast accuracy of wind power especially for short-term wind power prediction[12][13]. Even though more precise methods are proposed, the prediction error is still systemic and inherent in these methods[14] and some researchers try to learn from the historical prediction errors and make necessary modifications on the prediction results to improve the prediction[15]. Even though the deterministic prediction is still the main topic in wind power forecast, the inherent uncertainty of wind power prediction makes it extremely difficult to predict the wind power output precisely, which can potentially impact the day-ahead planning of the WHHPS[16]. Recently, the quantification of wind power forecast uncertainty has been attracting more attention[17]. Unlike the deterministic prediction, when considering the uncertainty, the probabilistic nature of wind power output is usually modelled by a probability distribution[18]. In probabilistic forecasting, the parametric density functions like Weibull probability density function[19], or non-parametric density functions using kernel density estimation[20] are the two main techniques to construct the predictive distributions.

As the probabilistic forecast is usually generated independently for every look-ahead time and does not take into account the spatial-temporal dependency, [21] makes efforts in considering spatial-temporal dependency prediction for electricity prices. However, a more widely adopted method for day-ahead planning is the scenario-based method[14]. Combining with stochastic optimization, an expected best day-ahead plan can be obtained given the representative scenarios of the wind power output.

Using the stochastic optimization is predicated on knowing these representative scenarios in advance[22]. Different researchers use different ways to generate the representative scenarios. One of the most common ways is to fit a

probability distribution, usually the Gaussian distribution, to the prediction error[23][24] and extract the representative scenarios through different sampling methods like Monte Carlo sampling and Latin hypercube sampling[11]. Then by adding the errors to the point forecast results, the representative scenarios of the wind power output can be obtained. Apart from this, [25] statistically analyses the fluctuation characteristics of adjacent time intervals of wind power and acquires representative scenarios of wind power output under a certain probability with the intervals to obtain the optimum generation schedule of hydropower with minimum water consumption. Ref. [26] uses machine learning-based methods to find the uncertainty rule inherent in the historical data to generate high quality wind power output representative scenarios for purposes of operations planning.

As shown above, there are many ways to handle the wind power for purposes of day-ahead planning, however, each method has its own limits. Using the deterministic prediction results to make the day-ahead plan directly fails to consider the possible prediction errors caused by forecast uncertainty, while the stochastic model aims to calculate an expected best plan across the space of all possible representative scenarios, however, to better depict the uncertainty, many representative scenarios are needed which may increase the computation burden[27].

There has already been a vast amount of research into the development and implementation of day-ahead planning in the context of short-term operational planning in wind-integrated hybrid power systems. However, there has been relatively little research conducted with the aim of properly gauge the performance of the day-ahead plans especially from the perspective of real-time operation (i.e., investigate the effectiveness of the day-ahead plan in real-time operation given any uncertainty).

Discussion of the day-ahead plan performance in real-time operation has been a commonly adopted way to prove the effectiveness of the plan in other research fields. In the context of short-term operational planning for power systems with high levels of wind power integration, the uncertainty inherent in the wind power forecast is also widely considered in the day-ahead planning framework. Comparing with the day-ahead plan for WHHPS, these plans made for power system operation are usually evaluated by comparing them to the the realised real-time operation profile of the power system. For example, to mitigate the impacts of prediction errors of regulation reserve requirements caused by the inherent uncertainty associated with wind power output forecasts, [17] proposes a day-ahead planning framework for the regulation reserve requirement under uncertainty with a given confidence level, and the results are compared with the actual regulation reserve realised in real-time operation.

Despite the need for evaluating the performance and effectiveness of day-ahead plans in real-time realization, most studies limit their methodologies to only studying the development of day-ahead planning profiles. For example, [11] discusses the comprehensive risk of the hydro-wind-photovoltaic complementary system with the day-ahead plans obtained from wind power representative scenarios set, whereas [27] proposes a hybrid robust-interval optimization approach for integrated energy system planning considering the uncertainty of RESs and demand, and the effectiveness of the proposed method is discussed under various probability levels. Ref. [28] proposes a stochastic optimization model to decrease the output shortage, power curtailment and spilled water risks in wind-solar-hydro complementary operation, and the ability of the proposed method in decreasing these risks is discussed in the generated representative scenarios for wind and PV power output. These studies neglect any comparison of the day-ahead profiles with realised real-time operation profiles.

To extend the discussion from day-ahead level into actual operation level, [29] proposes a robust optimization model that accounts for uncertain PV power generation to maximize the hydro-PV output while minimizing the water consumption. To this end, a representative day is selected to conduct the proposed model and the results are compared with historical actual operation data to show the efficiency of the proposed model. Ref. [30] proposes a multi-time scale optimal dispatch strategy combining robust optimization and rolling optimization for the combined cooling, heating and power microgrid containing renewable energy sources, and the effectiveness of the proposed model is showcased by comparing the operation cost in day-ahead plan and actual historical operation data. Even though the effectiveness of these proposed models is verified in actual operation level, these methods cannot be used to evaluate the day-ahead plan for the WHHPS that is going to be used in the coming real-time operation, in other words, these historical actual operation data comes from the plan made in advance and there is no way to gauge the performance of the day-ahead plan until it is executed in real-time operation. A proper method to evaluate the performance of the day-ahead plan for real-time operation is therefore still not available.

Consequently, there is still room to further investigate the methods to properly gauge the performance of a given day-ahead plan under real-time operation. Most research does not extend their studies into actual operation level nor these methods presented in existing literature is feasible for evaluating day-ahead plans from the perspective of real-time operation. The main reason for these shortcomings is that the criteria for day-ahead plan evaluation from perspective of real-time operation is not clear.

Some research has made some efforts to evaluate the day-ahead plan from the perspective of real-time operation. Ref. [26] demonstrates the effectiveness of a proposed scenario generation method by exploring its impact on hydropower start-stop times compared to the Gaussian copula method under the same objective. This might be a way to evaluate the day-ahead plan from the perspective of real-time operation, however, it is not practically valuable to ascertain a result that the plan leads to lower start-stop times is certainly better. Ref. [31] proposes three benefit indices and five risk indices to evaluate the day-head plan of the wind-PV-hydropower

hybrid power system from the perspective of real-time operation. This work contributes to the gap, however, no method is proposed to improve the performance of the day-head plan in these indices and the large evaluation index system is not convenient in practice.

To address all the problems mentioned above, we proposed a novel data-driven tighten-constraint method to improve the day-ahead plan and a metric to evaluate the day-ahead plan from the perspective of real-time operation. The effectiveness of the proposed method is verified by comparing it with alternative day-ahead planning frameworks and the suggestion in using the proposed method is given.

1.3. Contribution

The contributions of this paper are summarized as follows:

(1) A new data-driven tighten-constraint method to improve the performance of the day-ahead plan in real-time operation for WHHPS is proposed;
(2) A metric to evaluate the day-ahead plan from the perspective of real-time operation is proposed;
(3) A bilevel game theory based model is proposed to provide the data-driven base for the proposed adjustment parameter;
(4) Numerical results are provided to test the new method and give suggestions to improve the effectiveness of the proposed method.

2. WHHPS operation model

This section proposes the operation models of the WHHPS for both day-ahead planning and real-time operation. First, the procedure of short-term complementary operation of the WHHPS is briefly described and any underlying assumptions are explained in Section 2.1. Then the day-ahead planning model, real-time operation model and reliability metric are introduced in Sections 2.2 and 2.3, respectively. Furthermore, the models are reformulated in Section 2.4.

2.1. Problem description

Essentially the short-term complementary operation of the WHHPS is realised by two processes: 1) the day-ahead planning and 2) real-time operation. The detailed description of the relationship between these two processes can be found in [11] but a summary is given in this section. The WHHPS first considers its own operation objectives and determines a generation schedule for the following day based on its own resource forecast. This schedule is called the day-ahead plan. This plan will then be submitted to the SO and the confirmed plan will be returned to the WHHPS. On the day of the real-time operation, the WHHPS will schedule its resources to generate power according to the confirmed generation plan. To complete these two processes, two operation models are needed for both day-ahead planning and real-time operation, respectively. Before looking at the models, two assumptions are made as below:

(1) The day-ahead plan made by the WHHPS gets no revision from the SO;
(2) Only the wind power output forecast contains uncertainty, and the uncertainty in hydro inflow prediction is ignored[28].

2.2. The Day-ahead Planning Model

Given the fluctuating of wind resources, the output of the wind power fluctuates frequently and largely which prevents the wind power from easy utilisation by the SO. In the WHHPS, the hydropower can help to mitigate the risks of relying solely on the fluctuating wind power by compensating for its variations thereby creating an overall smooth output profile which in effect helps to maximise the integration of wind power [32]. Mathematically, considering a scheduling time horizon $\tau = \{1, \cdots, T\}$, the day-ahead planning model for a WHHPS is formulated as follows:

$$\text{Maximize} \sum_{t\in\tau\backslash\{T\}} N_t^d \cdot \Delta t \tag{1a}$$

$$\text{Minimize} \frac{\sum_{t\in\tau\backslash\{T\}}(N_t^d - \bar{N}^d)^2}{T-1} \tag{1b}$$

Subject to:

$$N_t^d = N_{h,t}^d + N_{w,t}^d \,:\, \gamma_{2,t}, \forall t \in \tau\backslash\{T\} \tag{1c}$$

$$\bar{N}^d = \frac{\sum_{t\in\tau\backslash\{T\}} N_t^d}{T-1} \,:\, \gamma_3 \tag{1d}$$

$$N_{w,t}^{min,d} \le N_{w,t}^d \le N_{w,t}^{max,d} \,:\, \underline{\mu_{1,t}}, \overline{\mu_{1,t}}, \forall t \in \tau\backslash\{T\} \tag{1e}$$

$$N_{h,t}^d = \frac{kQ_{g,t}^d h_t^d}{e_N}, \forall t \in \tau\backslash\{T\} \tag{1f}$$

$$N_{h,t}^{min} \le N_{h,t}^d \le N_{h,t}^{max}, \forall t \in \tau\backslash\{T\} \tag{1g}$$

$$h_t^d = \frac{Z_{u,t}^d + Z_{u,t+1}^d}{2} - Z_{d,t}^d - h_{l,t}^d \,:\, \gamma_{5,t}, \forall t \in \tau\backslash\{T\} \tag{1h}$$

$$Z_{d,t}^d = f^{QZ}(Q_{o,t}^d), \forall t \in \tau\backslash\{T\} \tag{1i}$$

$$Q_{o,t}^d = \frac{(V_t^d - V_{t+1}^d)}{3600\Delta t} + Q_{in,t} \,:\, \gamma_{7,t}, \forall t \in \tau\backslash\{T\} \tag{1j}$$

$$Q_{o,t}^{min} \le Q_{o,t}^d \le Q_{o,t}^{max} \,:\, \underline{\mu_{7,t}}, \overline{\mu_{7,t}}, \forall t \in \tau\backslash\{T\} \tag{1k}$$

$$Q_{g,t}^d \le Q_{o,t}^d \,:\, \mu_{8,t}, \forall t \in \tau\backslash\{T\} \tag{1l}$$

$$V_t^d = f^{ZV}(Z_{u,t}^d) \,:\, \forall t \in \tau \tag{1m}$$

$$Z_{u,t}^{min} \le Z_{u,t}^d \le Z_{u,t}^{max} \,:\, \underline{\mu_{9,t}}, \overline{\mu_{9,t}}, \forall t \in \tau\backslash\{T\} \tag{1n}$$

$$Z_{u,1}^d = Z_u^{ini} \,:\, \gamma_{10} \tag{1o}$$

$$Z_{u,T}^d = Z_u^{fin} \,:\, \gamma_{11} \tag{1p}$$

The WHHPS initiates with the aim to maximise the use of the renewable resources for power production and smoothing the output profile. These are shown with the objective functions (1a) and (1b), which denote the total generation and output fluctuation of the WHHPS over the whole scheduling periods, respectively. Eqs. (1c) and (1d) guarantee the output balance of the WHHPS. Eq. (1e) ensures the wind power output is within the predicted available power and its nominal

capacity. Eq. (1f) is the generation function for hydropower. There are many forms of hydropower generation function in the real world applications[33], and we follow [34] to choose the head independent constant energy conversion efficiency factors as the generation function. Eq. (1g) ensures the hydropower output is within its capacity and (1h) stands for the generation head for hydropower in each time period. Eqs. (1i) and (1m) are the reservoir characteristic curves for outflow and tailwater level, reservoir water level and reservoir volume, respectively. Eq. (1j) guarantees the hydropower water balance in each time period. Eq. (1k) ensures the outflow is within the allowed level and (1l) ensures the generation flow is no larger than the outflow in the same time period. Eq. (1n) ensures the reservoir works in its allowed water level all the time. Finally, (1o) and (1p) ensure the initial water level and final water level follow the operational instructions.

2.3. Real-time Operation Model and Reliability Metric

2.3.1. Real-time operation model

When the day-ahead plan is submitted to and accepted by the SO, the WHHPS is expected to operate according to the plan in real-time operation. However, as the actual available wind power may be different from that of the forecast wind power when making the day-ahead plan and the actual available output of wind power cannot be obtained in advance, in real-time operation, the WHHPS needs to redispatch period by period to follow the generation schedule.

Mathematically, this real-time operation process can be formulated as the following model:

$$\text{Minimize} \sum_{t\in\tau\backslash\{T\}} y_{r,t}\cdot R_t \tag{2a}$$

Subject to:

$$y_{r,t}\in\{0,1\}, \forall t\in\tau\backslash\{T\} \tag{2b}$$

$$1-\frac{N_t^r}{N_t^d}\le y_{r,t}, \forall t\in\tau\backslash\{T\} \tag{2c}$$

$$N_t^r = N_{h,t}^r + N_{w,t}^{max,r}, \forall t\in\tau\backslash\{T\} \tag{2d}$$

$$N_{h,t}^r \le max\{0, N_t^d - N_{w,t}^{max,r}\}, \forall t\in\tau\backslash\{T\} \tag{2e}$$

$$\text{Constraints(1f)}-\text{(1p)} \text{ with the '}d\text{' in the superscript replaced by '}r\text{'.} \tag{2f}$$

where $y_{r,t}$ is a binary variable indicating if the generation plan in the period t is not fulfilled in real-time redispatch, when $N_t^r < N_t^d$, $y_{r,t} = 1$. R_t is a predefined parameter for the period t. The later the period t is, the smaller the R_t should be. This can guarantee the preceding period gets the priority over the latter periods in fulfillment. For example, $R_t \ge \sum_{b\in B(t)} R_b + 1$, where $B(t)$ is the set for periods later than period t.

The objective function (2a) minimizes the number of unfulfilled preceding periods, which guarantee the WHHPS operates period by period. Eqs. (2b) and (2c) ensure there are only two states for each time period, i.e. fulfilled or unfulfilled, whereas (2d) is the real-time available output of WHHPS in each time period. Eq. (2e) ensures the WHHPS will not generate power exceeding that of the scheduled power in the day-ahead plan. Finally, (2f) achieves the same effects as in the day-ahead planning model.

2.3.2. Reliability metric

If the wind power output can be obtained with 100% certainty, the day-ahead plan can be executed perfectly in real-time operation. However, with the inherent uncertainty in day-ahead wind power prediction, the actual realised real-time operation profile may be quite different and therefore the expected effectiveness of the hybrid power system in the plan may not necessarily be achieved. Therefore, it is imperative to evaluate how day-ahead plans actually perform from the perspective of real-time operation. However, as mentioned in introduction, most of the research only focuses on day-ahead planning, and few extend the analysis of the day-ahead plan of the hybrid power system into real-time operation which makes this problem still under explored. We think the main reason is the lack of a viable mathematical method to evaluate the performance of the day-ahead plan from the perspective of real-time operation. To handle this gap, we propose a metric in this paper.

After receiving the confirmed plan, the WHHPS is expected to operate according to the plan in real-time operation. With the inherent uncertainty in the wind power prediction, it might be difficult to fulfill the generation schedule made in the day-ahead plan exactly in real-time operation, and therefore the reliability is proposed as a metric to show the completion status of the day-ahead plan:

$$\mathbb{R} = \frac{\sum_{t\in\tau\backslash\{T\}}(1-y_{r,t})N_t^d}{\sum_{t\in\tau\backslash\{T\}} N_t^d} \tag{3}$$

For a day-ahead plan, $\mathbb{R}\in[0,1]$. When the $\mathbb{R}=1$, the day-ahead plan is reliable.

2.4. Reformulation

Even though in the previous sections, the mathematical models for day-ahead planning and real-time operation have been proposed, there still remain two problems namely, (1) the day-ahead planning model is a multi-objective model which leads to a solution of Pareto front, which is therefore practically not viable. As stated in Section 2.1, the WHHPS can only submit one plan to the SO and (2) influenced by the bilinear terms in (1f), and the expression of the functions in (1i) and (1m), the day-ahead planning model and real-time operation model are non-convex and difficult to solve. Therefore, before going any further, the reformulation of these two models is detailed below.

2.4.1. ε-constraint method for multi-objective model

As only one plan is needed in day-ahead planing process, only one function can be set as the objective. There are

mainly two ways to reformulate the multi-objective model into single-objective model, i.e. scalarization[35] and ε-constraint method[36]. As the two objectives in this model are in different magnitudes, when merging the two objectives into a single scalar function, it is difficult to pre-define the weight vector for them. Meanwhile, it is hard to explain the inherent meaning of the plan made from the scalar function. On the contrary, the latter method has a clear and more explainable nature by transforming the objective into constraint. Thus, the ε-constraint method is chosen to reformulate (1b) as (4a).

$$\frac{\sum_{t\in\tau\backslash\{T\}}(N_t^d - \bar{N}^d)^2}{T-1} \leq \varepsilon \tag{4a}$$

where ε is the predefined parameter by the following optimization problem:

$$\varepsilon = \theta \cdot \text{Maximize} \frac{\sum_{t\in\tau\backslash\{T\}} (\grave{N_{w,t}} - \bar{N}_w)^2}{T-1} \tag{4b}$$

$$\bar{N}_w = \frac{\sum_{t\in\tau\backslash\{T\}} \grave{N_{w,t}}}{T-1} \tag{4c}$$

$$N_{w,t}^{min} \leq \grave{N_{w,t}} \leq N_w^{cap}, \forall t \in \tau\backslash\{T\} \tag{4d}$$

where $\grave{N_{w,t}}$ is the wind power output at period t. $\bar{N}_w$ is the average of wind power output profile. θ is the predetermined non-negative parameter which is not larger than 1. N_w^{cap} is nominal capacity of the wind power generator. In this research we choose a fluctuation averse strategy in hope of an absolutely smoothed output profile from the WHHPS. By setting the θ to be 0, the (4a) can further be replaced by (4e).

$$N_t^d - \bar{N}^d = 0 : \gamma_{1,t}, \forall t \in \tau\backslash\{T\} \tag{4e}$$

2.4.2. Linearization of constraints

To further simplify the model, first, we follow [37] to set the function expressions in (1i) and (1m) as (4h) and (4f)-(4g), respectively. Further, the McCormick convex relaxation[38] is used to relax the the product of terms in (1f) as (4i)-(4m).

$$V_t^d = \zeta^{ZV} \cdot Z_{u,t}^d + \xi^{ZV} : \gamma_{8,t}, \forall t \in \tau\backslash\{T\} \tag{4f}$$

$$V_T^d = \zeta^{ZV} \cdot Z_{u,T}^d + \xi^{ZV} : \gamma_9 \tag{4g}$$

$$Z_{d,t}^d = \zeta^{QZ} \cdot Q_{o,t}^d + \xi^{QZ} : \gamma_6, \forall t \in \tau\backslash\{T\} \tag{4h}$$

$$N_{h,t}^d = \frac{kW_t^d}{e_N} : \gamma_{4,t}, \forall t \in \tau\backslash\{T\} \tag{4i}$$

$$W_t^d \geq Q_g^{\min} h_t^d + h^{\min} Q_{g,t}^d - Q_g^{\min} h^{\min} : \mu_{2,t}, \forall t \in \tau\backslash\{T\} \tag{4j}$$

$$W_t^d \geq Q_g^{\max} h_t^d + h^{\max} Q_{g,t}^d - Q_g^{\max} h^{\max} : \mu_{3,t}, \forall t \in \tau\backslash\{T\} \tag{4k}$$

$$W_t^d \leq Q_g^{\max} h_t^d + h^{\min} Q_{g,t}^d - Q_g^{\max} h^{\min} : \mu_{4,t}, \forall t \in \tau\backslash\{T\} \tag{4l}$$

$$W_t^d \leq Q_g^{\min} h_t^d + h^{\max} Q_{g,t}^d - Q_g^{\min} h^{\max} : \mu_{5,t}, \forall t \in \tau\backslash\{T\} \tag{4m}$$

After these treatments, the day-ahead planning model and real-time operation model are reformulated as LP problem and MIP problem, respectively.

3. Tighten-constraint method

This section proposes the tighten-constraint method for reliability improvement of the day-ahead plan. Specifically, the tightened constraint with adjustment parameter is presented in Section 3.1. Then, a bilevel optimization problem is proposed to obtain the adjustment parameter in Section 3.2. Further, in Section 3.3, we detail the treatment of the bilevel optimization problem, which is reformulated as a MILP problem.

3.1. Tightened constraint with adjustment parameter

In the WHHPS, hydropower plant is the main regulation tool to handle the fluctuation of wind power while achieving the operation objective. However, with the forecast uncertainty in wind power, high expectations in the day-ahead plan can lead to failure during the implementation in the next day. This is primarily caused by two main reasons namely, 1) the forecast wind power is higher than real-time available wind power, which results in a relative shortfall of energy, and 2) the hydropower plant utilized its entire dispatching capacity when making the day-ahead plan in pursuit of higher smooth output of the WHHPS. To overcome these two issues, we introduce the adjustment parameter λ_t into (1g) as follows:

$$N_{h,t}^{min} \leq N_{h,t}^d \leq \lambda_t N_{h,t}^{max} : \underline{\mu_{6,t}}, \overline{\mu_{6,t}}, \forall t \in \tau\backslash\{T\} \tag{5}$$

3.2. Bilevel Stackelberg model

By introducing the adjustment parameter, a day-ahead plan with high reliability and high smooth output profile is expected. This can be interpreted as a single leader single follower bilevel Stackelberg model where real-time operation acts as the leader and day-ahead planning model is the follower[39]. In particular, the leader operates according to the day-ahead plan and decides the adjustment parameter at the upper level. Subsequently, the follower reacts to the adjustment parameter to make the day-ahead plan considering their own objective at the lower level. Specifically, the real-time operation maximizes the fulfilled generation by setting the adjustment parameter. And the day-ahead planning model tries to make a high smooth generation plan after receiving the adjustment parameter and return the plan for real-time operation. As a result, the optimum adjustment parameter for a high reliability and high smooth output profile in day-ahead plan can be obtained. The presentation of the bilevel model is inspired by [40].

3.2.1. Leader's problem

The first aim of the leader is to maximize the reliability of the day-ahead plan. However, to improve the reliability of the

day-ahead plan, the leader tends to minimize the adjustment parameter, which means that it forces the follower to make a smaller generation plan. Under the specified initial and final reservoir water levels, high water curtailment may occur which will result in energy loss. Consequently, the second aim is to maximize the output in real-time operation. Mathematically, the leader's objectives can be modeled as follows:

$$\underset{\Xi_{leader}}{\text{Maximize}} \frac{\sum_{t\in\tau\backslash\{T\}}(1-y_{r,t})N_t^d}{\sum_{t\in\tau\backslash\{T\}} N_t^d} \tag{6a}$$

$$\underset{\Xi_{\text{leader}}}{\text{Maximize}} \sum_{t\in\tau\backslash\{T\}} (1-y_{r,t})N_t^d \Delta t \tag{6b}$$

Again, with the help of ε-constraint method, the objective (6a) is transformed into constraint and the leader's problem is fully illustrated as:

$$\underset{\Xi_{\text{leader}}}{\text{Maximize}} \sum_{t\in\tau\backslash\{T\}} N_t^d \Delta t \tag{6c}$$

Subject to:

$$0 \le \lambda_t \le 1, \forall t \in \tau\backslash\{T\} \tag{6d}$$

$$N_t^r \ge N_t^d, \forall t \in \tau\backslash\{T\} \tag{6e}$$

$$\text{Constraints (2d), (4i)} - \text{(4m), (1g), (1h), (4h), (1j)} - \text{(1l), (4f), (4g), (1n)} - \text{(1p)}$$
with the 'd' in the superscript replaced by 'r'. (6f)

The decision variables of the leader problem are $\Xi_{\text{leader}} = \{\lambda_t, N_t^r, N_{h,t}^r, W_t^r, h_t^r, Q_{g,t}^r, Z_{u,t}^r, Z_{d,t}^r, h_{l,t}^r, Q_{o,t}^r, V_t^r, Z_{u,T}^r, V_T^r, \forall t \in \tau\backslash\{T\}\}$. The leader objective function (6c) denotes the generation in real-time operation. When setting the ε for objective (6a) as 1, the generation in real-time operation is equal to day-ahead planned generation. Eq. (6d) constrains the adjustment parameter decision of the leader. Eq. (6e) guarantees the completion of the day-ahead generation schedule in real-time operation in each time period. Eq. (6f) works the same as in previous models.

3.2.2. Follower's Model

The follower in the bilevel Stackelberg model makes the day-ahead plan with the tightened constraint after getting the adjustment parameter from the leader. A high smooth generation plan is considered as the follower's problem. The follower's problem is modeled as follows:

$$\underset{\Xi_{follower}}{\text{Maximize}}\text{(1a)} \tag{7a}$$

Subject to:

$$\text{Constraints (4e), (1c)} - \text{(1e), (4i)} - \text{(4m), (5), (1h), (4h), (1j)} - \text{(1l), (4f), (4g), (1n)} - \text{(1p).} \tag{7b}$$

Where $\Xi_{follower} = \{N_t^d, \bar{N}^d, N_{h,t}^d, N_{w,t}^d, W_t^d, h_t^d, Q_{g,t}^d, Z_{u,t}^d, Z_{d,t}^d, h_{l,t}^d, Q_{o,t}^d, V_t^d, V_T^d, Z_{u,T}^d, \forall t \in \tau\backslash\{T\}\}$ is the decision variables for the follower. $\Xi_{follower}^{dual} = \{\gamma_{1,t}, \gamma_{2,t}, \gamma_3, \underline{\mu_{1,t}}, \overline{\mu_{1,t}}, \gamma_{4,t}, \mu_{2,t}, \mu_{3,t}, \mu_{4,t}, \mu_{5,t}, \underline{\mu_{6,t}}, \overline{\mu_{6,t}}, \gamma_{5,t}, \gamma_{6,t}, \gamma_{7,t}, \underline{\mu_{7,t}}, \overline{\mu_{7,t}}, \mu_{8,t}, \gamma_{8,t}, \gamma_9, \underline{\mu_{9,t}}, \overline{\mu_{9,t}}, \gamma_{10}, \gamma_{11}, \forall t \in \tau\backslash\{T\}\}$ represents the set of dual variables of the corresponding constraints in the follower's problem.

3.2.3. Bilevel model

After formulating both the leader's and follower's problems, the proposed bilevel Stackelberg model for a scenario day can be summarized as follows.

$$\Xi_{leader} \in \arg \underset{\Xi_{\text{leader}}}{\text{Maximize}}\text{(6c)} \tag{8a}$$

Subject to:

$$\text{Constraints(6d)} - \text{(6f)} \tag{8b}$$

$$\Xi_{follower}, \gamma_{1,t}, \gamma_{2,t}, \gamma_3, \underline{\mu_{1,t}}, \overline{\mu_{1,t}}, \gamma_{4,t}, \mu_{2,t}, \mu_{3,t}, \mu_{4,t}, \mu_{5,t}, \underline{\mu_{6,t}}, \overline{\mu_{6,t}}, \gamma_{5,t}, \gamma_{6,t}, \gamma_{7,t}, \underline{\mu_{7,t}}, \overline{\mu_{7,t}}, \mu_{8,t}, \gamma_{8,t}, \gamma_9, \underline{\mu_{9,t}}, \overline{\mu_{9,t}}, \gamma_{10}, \gamma_{11}$$
$$\in \arg \underset{\Xi_{follower}}{\text{Maximize}}\{\text{(7a)}$$
Subject to:
$$\text{Constraint (7b)}\}, \forall t \in \tau\backslash\{T\} \tag{8c}$$

This is a single-leader-single-follower Stacklberg game model. Eqs. (8a) and (8b) denote the real-time operation in the upper level while (8c) represents the reaction of the day-ahead planning given by the upper level decision. The methods to solve the bilevel Stacklberg game model are discussed in detail next.

3.3. Solution methods

The proposed bilelve model in Section 3.2.3 is challenging to solve due to the mutual influence of the upper and lower levels' models. In this section, first, the bilevel model is transferred into a single-level model. Then, the single-level model is linearized and reformulated as a MILP.

3.3.1. Single-level model transformation

As the lower level problem is a LP problem, the strong duality can be guaranteed. The KKT optimality conditions of the lower level problem can be derived to transform the bilevel model into a single-level model. The single-level model is shown below:

$$\underset{\Xi_{\text{single}}}{\text{Maximize}}\text{(6c)} \tag{9a}$$

Subject to:

$$\text{Constraint(8b)} \tag{9b}$$

$$-\Delta t+\gamma_{1,t}+\gamma_{2,t}-\frac{\gamma_3}{T-1}=0,\forall t\in\tau\backslash\{T\} \tag{9c}$$

$$\gamma_3-\sum_{t\in\tau\backslash\{T\}}\gamma_{1,t}=0 \tag{9d}$$

$$-\underline{\mu_{6,t}}+\overline{\mu_{6,t}}-\gamma_{2,t}+\gamma_{4,t}=0,\forall t\in\tau\backslash\{T\} \tag{9e}$$

$$-\underline{\mu_{1,t}}+\overline{\mu_{1,t}}-\gamma_{2,t}=0,\forall t\in\tau\backslash\{T\} \tag{9f}$$

$$-\mu_{2,t}-\mu_{3,t}+\mu_{4,t}+\mu_{5,t}-\frac{\gamma_{4,t}k}{e_N}=0,\forall t\in\tau\backslash\{T\} \tag{9g}$$

$$\mu_{2,t}Q_g^{\min}+\mu_{3,t}Q_g^{\max}-\mu_{4,t}Q_g^{\max}-\mu_{5,t}Q_g^{\min}+\gamma_{5,t}=0,\ \forall t\in\tau\backslash\{T\} \tag{9h}$$

$$\mu_{2,t}h^{\min}+\mu_{3,t}h^{\max}-\mu_{4,t}h^{\min}-\mu_{5,t}h^{\max}+\mu_{8,t}=0,\ \forall t\in\tau\backslash\{T\} \tag{9i}$$

$$-\underline{\mu_{9,t}}+\overline{\mu_{9,t}}-\frac{\gamma_{5,t}}{2}-\gamma_{8,t}\zeta^{ZV}=0,\forall t\in\tau\backslash\{T\} \tag{9j}$$

$$\gamma_{5,t}+\gamma_{6,t}=0,\forall t\in\tau\backslash\{T\} \tag{9k}$$

$$\gamma_{5,t}=0,\forall t\in\tau\backslash\{T\} \tag{9l}$$

$$-\underline{\mu_{7,t}}+\overline{\mu_{7,t}}-\mu_{8,t}-\gamma_{6,t}\zeta^{QZ}+\gamma_{7,t}=0,\forall t\in\tau\backslash\{T\} \tag{9m}$$

$$-\frac{\gamma_{7,t}}{3600\Delta t}+\gamma_{8,t}=0,\forall t\in\tau\backslash\{T\} \tag{9n}$$

$$N_t^d-\bar{N}^d=0,\forall t\in\tau\backslash\{T\} \tag{9o}$$

$$N_t^d-N_{h,t}^d-N_{w,t}^d=0,\forall t\in\tau\backslash\{T\} \tag{9p}$$

$$\bar{N}^d-\frac{\sum_{t\in\tau\backslash\{T\}}N_t^d}{T-1}=0 \tag{9q}$$

$$0\le(N_{w,t}^d-N_{w,t}^{min,d})\perp\underline{\mu_{1,t}}\ge0,\forall t\in\tau\backslash\{T\} \tag{9r}$$

$$0\le(N_{w,t}^{max,d}-N_{w,t}^d)\perp\overline{\mu_{1,t}}\ge0,\forall t\in\tau\backslash\{T\} \tag{9s}$$

$$0\le(W_t^d-Q_g^{\min}h_t^d-h^{\min}Q_{g,t}^d+Q_g^{\min}h^{\min})\perp\mu_{2,t}\ge0,\ \forall t\in\tau\backslash\{T\} \tag{9t}$$

$$0\le(W_t^d-Q_g^{\max}h_t^d-h^{\max}Q_{g,t}^d+Q_g^{\max}h^{\max})\perp\mu_{3,t}\ge0,\ \forall t\in\tau\backslash\{T\} \tag{9u}$$

$$0\le(Q_g^{\max}h_t^d+h^{\min}Q_{g,t}^d-Q_g^{\max}h^{\min}-W_t^d)\perp\mu_{4,t}\ge0,\ \forall t\in\tau\backslash\{T\} \tag{9v}$$

$$0\le(Q_g^{\min}h_t^d+h^{\max}Q_{g,t}^d-Q_g^{\min}h^{\max}-W_t^d)\perp\mu_{5,t}\ge0,\ \forall t\in\tau\backslash\{T\} \tag{9w}$$

$$0\le(N_{h,t}^d-N_{h,t}^{min})\perp\underline{\mu_{6,t}}\ge0,\forall t\in\tau\backslash\{T\} \tag{9x}$$

$$0\le(\lambda_tN_{h,t}^{max}-N_{h,t}^d)\perp\overline{\mu_{6,t}}\ge0,\forall t\in\tau\backslash\{T\} \tag{9y}$$

$$0\le(Q_{o,t}^d-Q_{o,t}^{min})\perp\underline{\mu_{7,t}}\ge0,\forall t\in\tau\backslash\{T\} \tag{9z}$$

$$0\le(Q_{o,t}^{max}-Q_{o,t}^d)\perp\overline{\mu_{7,t}}\ge0,\forall t\in\tau\backslash\{T\} \tag{9aa}$$

$$0\le(Q_{o,t}^d-Q_{g,t}^d)\perp\mu_{8,t}\ge0,\forall t\in\tau\backslash\{T\} \tag{9ab}$$

$$0\le(Z_{u,t}^d-Z_{u,t}^{min})\perp\underline{\mu_{9,t}}\ge0,\forall t\in\tau\backslash\{T\} \tag{9ac}$$

$$0\le(Z_{u,t}^{max}-Z_{u,t}^d)\perp\overline{\mu_{9,t}}\ge0,\forall t\in\tau\backslash\{T\} \tag{9ad}$$

$$N_{h,t}^d-\frac{kW_t^d}{e_N}=0,\forall t\in\tau\backslash\{T\} \tag{9ae}$$

$$h_t^d-\frac{Z_{u,t}^d+Z_{u,t+1}^d}{2}+Z_{d,t}^d+h_{l,t}^d=0,\forall t\in\tau\backslash\{T\} \tag{9af}$$

$$Z_{d,t}^d-\zeta^{QZ}Q_{o,t}^d-\xi^{QZ}=0,\forall t\in\tau\backslash\{T\} \tag{9ag}$$

$$Q_{o,t}^d-\frac{(V_t^d-V_{t+1}^d)}{3600\Delta t}-Q_{in,t}=0,\forall t\in\tau\backslash\{T\} \tag{9ah}$$

$$V_t^d-\zeta^{ZV}Z_{u,t}^d-\xi^{ZV}=0,\forall t\in\tau \tag{9ai}$$

$$Z_{u,1}^d=Z_u^{ini} \tag{9aj}$$

$$Z_{u,T}^d=Z_u^{fin} \tag{9ak}$$

Where the decision variables of the single level problem are $\Xi_{single}=\{\lambda_t,N_t^r,N_{h,t}^r,W_t^d,h_t^r,Q_{g,t}^r,Z_{u,t}^r,Z_{d,t}^r,h_{l,t}^r,Q_{o,t}^r,V_t^r,Z_{u,T}^r,V_T^r,N_t^d,\bar{N}^d,N_{h,t}^d,N_{w,t}^d,W_t^d,h_t^d,Q_{g,t}^d,Z_{u,t}^d,Z_{d,t}^d,h_{l,t}^d,Q_{o,t}^d,V_t^d,V_T^d,Z_{u,T}^d,\gamma_{1,t},\gamma_{2,t},\gamma_3,\underline{\mu_{1,t}},\overline{\mu_{1,t}},\gamma_{4,t},\mu_{2,t},\mu_{3,t},\mu_{4,t},\mu_{5,t},\underline{\mu_{6,t}},\overline{\mu_{6,t}},\gamma_{5,t},\gamma_{6,t},\gamma_{7,t},\underline{\mu_{7,t}},\overline{\mu_{7,t}},\mu_{8,t},\gamma_{8,t},\gamma_9,\underline{\mu_{9,t}},\overline{\mu_{9,t}},\gamma_{10},\gamma_{11},\forall t\in\tau\backslash\{T\}\}$.

Eq. (9a) denotes the objective function of the single-level model. Eq. (9b) is the collection of constraints from the leader's model. Eqs. (9c)-(9n) are stationary conditions of the KKT optimality conditions. Eqs. (9o)-(9ak) are the primal feasible conditions, while (9r)-(9ad) represent the dual feasible and complementary slackness.

3.3.2. Linearization of the single-level model

Due to the product of variables in complementary slackness, the single-level model is non-convex. The Fortuny-Amat transformation is used by introducing an additional binary variable and a relatively large integer constant M[41]. The constraints of (9r)-(9ad) are linearized as (10a)-(10aa).

$$0\le N_{w,t}^d-N_{w,t}^{\min,d}\le(1-\underline{y_{1,t}})M,\forall t\in\tau\backslash\{T\} \tag{10a}$$

$$0\le\underline{\mu_{1,t}}\le\underline{y_{1,t}}M,\forall t\in\tau\backslash\{T\} \tag{10b}$$

$$0\le N_{w,t}^{max,d}-N_{w,t}^d\le(1-\overline{y_{1,t}})M,\forall t\in\tau\backslash\{T\} \tag{10c}$$

$$0\le\overline{\mu_{1,t}}\le\overline{y_{1,t}}M,\forall t\in\tau\backslash\{T\} \tag{10d}$$

$$0\le W_t^d-Q_g^{\min}h_t^d-h^{\min}Q_{g,t}^d+Q_g^{\min}h^{\min}\le(1-y_{2,t})M,\ \forall t\in\tau\backslash\{T\} \tag{10e}$$

$$0\le\mu_{2,t}\le y_{2,t}M,\forall t\in\tau\backslash\{T\} \tag{10f}$$

$$0\le W_t^d-Q_g^{\max}h_t^d-h^{\max}Q_{g,t}^d+Q_g^{\max}h^{\max}\le(1-y_{3,t})M,\ \forall t\in\tau\backslash\{T\} \tag{10g}$$

$$0\le\mu_{3,t}\le y_{3,t}M,\forall t\in\tau\backslash\{T\} \tag{10h}$$

$$0 \le Q_g^{\max} h_t^d + h^{\min} Q_{g,t}^d - Q_g^{\max} h^{\min} - W_t^d \le (1 - y_{4,t})M, \quad \forall t \in \tau \backslash \{T\} \tag{10i}$$

$$0 \le \mu_{4,t} \le y_{4,t} M, \forall t \in \tau \backslash \{T\} \tag{10j}$$

$$0 \le Q_g^{\min} h_t^d + h^{\max} Q_{g,t}^d - Q_g^{\min} h^{\max} - W_t^d \le (1 - y_{5,t})M, \quad \forall t \in \tau \backslash \{T\} \tag{10k}$$

$$0 \le \mu_{5,t} \le y_{5,t} M, \forall t \in \tau \backslash \{T\} \tag{10l}$$

$$0 \le N_{h,t}^d - N_{h,t}^{min} \le (1 - \underline{y_{6,t}})M, \forall t \in \tau \backslash \{T\} \tag{10m}$$

$$0 \le \underline{\mu_{6,t}} \le \underline{y_{6,t}} M, \forall t \in \tau \backslash \{T\} \tag{10n}$$

$$0 \le \lambda_t N_{h,t}^{max} - N_{h,t}^d \le (1 - \overline{y_{6,t}})M, \forall t \in \tau \backslash \{T\} \tag{10o}$$

$$0 \le \overline{\mu_{6,t}} \le \overline{y_{6,t}} M, \forall t \in \tau \backslash \{T\} \tag{10p}$$

$$0 \le Q_{o,t}^d - Q_{o,t}^{min} \le (1 - \underline{y_{7,t}})M, \forall t \in \tau \backslash \{T\} \tag{10q}$$

$$0 \le \underline{\mu_{7,t}} \le \underline{y_{7,t}} M, \forall t \in \tau \backslash \{T\} \tag{10r}$$

$$0 \le Q_{o,t}^{max} - Q_{o,t}^d \le (1 - \overline{y_{7,t}})M, \forall t \in \tau \backslash \{T\} \tag{10s}$$

$$0 \le \overline{\mu_{7,t}} \le \overline{y_{7,t}} M, \forall t \in \tau \backslash \{T\} \tag{10t}$$

$$0 \le Q_{o,t}^d - Q_{g,t}^d \le (1 - y_{8,t})M, \forall t \in \tau \backslash \{T\} \tag{10u}$$

$$0 \le \mu_{8,t} \le y_{8,t} M, \forall t \in \tau \backslash \{T\} \tag{10v}$$

$$0 \le Z_{u,t}^d - Z_{u,t}^{min} \le (1 - \underline{y_{9,t}})M, \forall t \in \tau \backslash \{T\} \tag{10w}$$

$$0 \le \underline{\mu_{9,t}} \le \underline{y_{9,t}} M, \forall t \in \tau \backslash \{T\} \tag{10x}$$

$$0 \le Z_{u,t}^{max} - Z_{u,t}^d \le (1 - \overline{y_{9,t}})M, \forall t \in \tau \backslash \{T\} \tag{10y}$$

$$0 \le \overline{\mu_{9,t}} \le \overline{y_{9,t}} M, \forall t \in \tau \backslash \{T\} \tag{10z}$$

$$\underline{y_{1,t}}, \overline{y_{1,t}}, y_{2,t}, y_{3,t}, y_{4,t}, y_{5,t}, \underline{y_{6,t}}, \overline{y_{6,t}}, \underline{y_{7,t}}, \overline{y_{7,t}}, y_{8,t}, \underline{y_{9,t}}, \overline{y_{9,t}} \in \{0, 1\}, \forall t \in \tau \backslash \{T\} \tag{10aa}$$

3.3.3. MILP problem and data-driven process

After the linearization, the single-level model is reformulated into a MILP problem that can be solved efficiently by commercial solvers. The complete MILP model is formulated as follows.

$$\underset{\Xi_{\text{MILP}}}{\text{Maximize}} (9a) \tag{11a}$$

Subject to:

$$\text{Constraints} (9b) - (9q), (10a) - (10aa), (9ae) - (9ak) \tag{11b}$$

Where the decision variables for the MILP model are $\Xi_{\text{MILP}} = \{\lambda_t, N_t^r, N_{h,t}^r, W_t^r, h_t^r, Q_{g,t}^r, Z_{u,t}^r, Z_{d,t}^r, h_{l,t}^r, Q_{o,t}^r, V_t^r, Z_{u,T}^r, V_T^r, N_t^d, \bar{N}^d, N_{h,t}^d, N_{w,t}^d, W_t^d, h_t^d, Q_{g,t}^d, Z_{u,t}^d, Z_{d,t}^d, h_{l,t}^d, Q_{o,t}^d, V_t^d, V_T^d, Z_{u,T}^d, \gamma_{1,t}, \gamma_{2,t}, \gamma_3, \underline{\mu_{1,t}}, \overline{\mu_{1,t}}, \gamma_{4,t}, \mu_{2,t}, \mu_{3,t}, \mu_{4,t}, \mu_{5,t}, \underline{\mu_{6,t}}, \overline{\mu_{6,t}}, \gamma_{5,t}, \gamma_{6,t}, \gamma_{7,t}, \underline{\mu_{7,t}}, \overline{\mu_{7,t}}, \mu_{8,t}, \gamma_{8,t}, \gamma_9, \underline{\mu_{9,t}}, \overline{\mu_{9,t}}, \gamma_{10}, \gamma_{11}, y_{1,t}, \overline{y_{1,t}}, y_{2,t}, y_{3,t}, y_{4,t}, y_{5,t}, \underline{y_{6,t}}, \overline{y_{6,t}}, \underline{y_{7,t}}, \overline{y_{7,t}}, y_{8,t}, \underline{y_{9,t}}, \overline{y_{9,t}}, \forall t \in \tau \backslash \{T\}\}$.

Taking a day as a scenario, all the training scenario days contain both day-ahead wind power output forecast and real-time actual wind power output. And the optimal adjustment parameter for these training scenario days can be obtained through the MILP problem. Moreover, taking the predicted wind power output, hydro inflow as inputs and corresponding adjustment parameter as output, a machine learning training and validating set can be generated. With the trained machine learning model, when making the day-ahead plan for practical use, using the wind power output forecast and hydro inflow information as input, a corresponding adjustment parameter to tighten the constraint for day-ahead planning model can be generated. The WHHPS can make the day-ahead plan and real-time operate with the normal processes, and the day-ahead plan can be evaluated by the proposed reliability metric. The complete procedure for the proposed method is shown in Fig.1.

4. Case study

In this case study, the effectiveness of the proposed tighten-constraint method is discussed. The WHHPS in this case study consists of a wind power generator and a hydropower generator as shown in Table 1. The entire scheduling period in the day-ahead planning framework and the subsequent real-time operation is 24 hours. A-year-long forecast and actual wind power output data of 4 wind power generators with 1h time intervals are obtained from [42]. A hydropower located in China is chosen and the inflow data is collected for the same days. The data is scaled to ensure the validity of the WHHPS in this case study. By replacing the wind power generator data in the WHHPS and taking each calendar day as a scenario, there are 1464 scenario days in total for this case study. Considering the consistency of the hydropower operation, the initial and final reservoir water levels are set as the same.

As the performance of different relaxing methods depends on the specific problem structure and data[37], for the WHHPS in this paper, with the testing method proposed in Appendix A, we use 10000 points to test the relaxation accuracy of the McCormick convex relaxation and the results show that an accuracy of more than 92.5% can be guaranteed in this case study. Apart from the control model, as mentioned in the introduction, stochastic model is the main method to handle the inherent uncertainty in wind power forecast. The models tested in this case study for comparison are listed in Table 2. The day-ahead plans for comparison are made with each method, and the real-time operation operates according to real-time operation model in Section 2.3. All the optimization problems in this paper are modeled in AIMMS and solved by Gurobi. The hardware environment of this paper is a personal computer with an Intel(R) Core(TM) i7-8700 CPU @ 3.20GHz 32GB RAM.

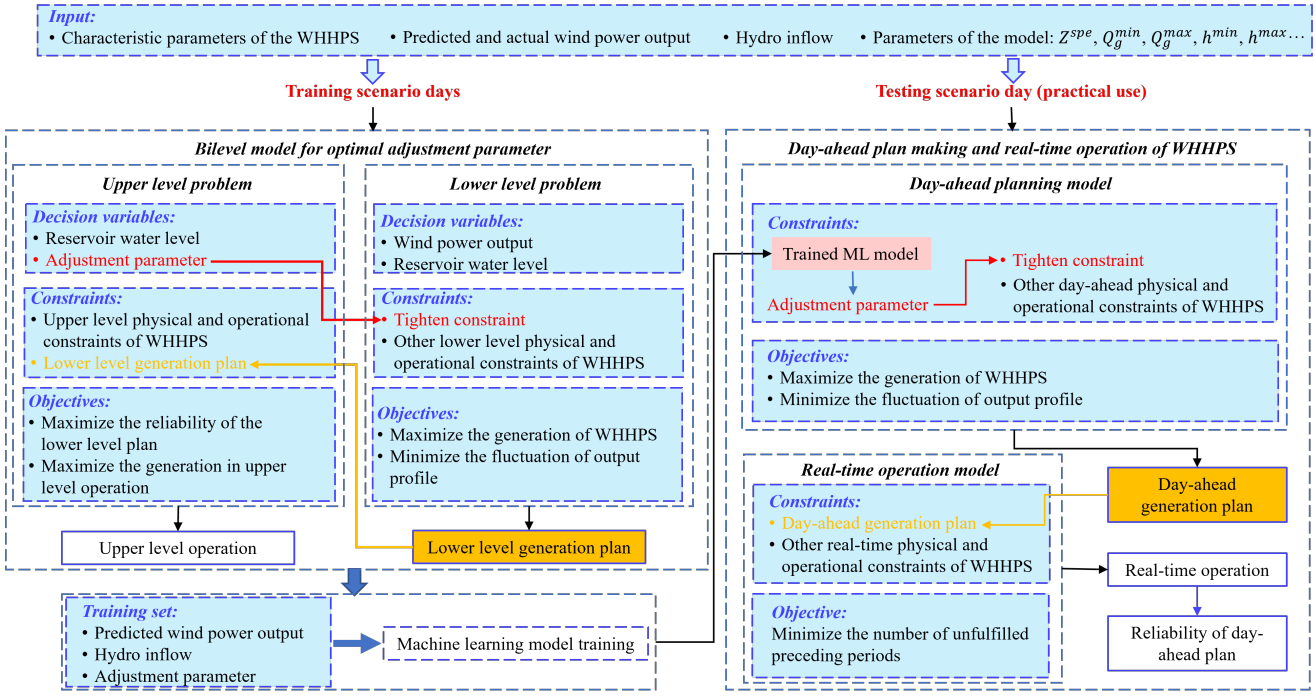

Figure 1: The complete procedure for the proposed method

Table 1
Parameter settings for WHHPS

Component	Parameter	Value	Unit
Wind power	Installed capacity	150	MW
Hydropower	Installed capacity	360	MW
	Dead water level	415	m
	Normal water level	425	m
	Maximum generation flow	589	m^3/s
	Maximum hydraulic head	91.5	m
	Minimum hydraulic head	73.75	m

4.1. Relationship between hydropower reservoir status and day-ahead plan reliability

4.1.1. Experimental step

In this section, the full 1464 scenario days are divided into training set with 1200 scenario days and testing set with 264 scenario days. The control model M1 is used as benchmark and as M5-M13 all contain our proposed method, we use M10 as a candidate to show the effectiveness of our proposed method under different hydropower reservoir status and the impact of the hydropower reservoir status on the results. We set 3 different initial and final reservoir water levels, i.e. 20%(417m), 50%(420m), 90%(424m) of the feasible water level range, to simulate different status of the hydropower reservoir as shown in Table 3. The adjustment parameters for the training set are obtained with the MILP in Section 3.3.3 and the results are used to train the XGBoost model in M10. The compared results are obtained by using the testing set as the testing scenario days for the M1 and M10.

4.1.2. The influence of different hydropower reservoir status under M1

Fig. 2 presents the planned generation for each scenario day under different hydropower reservoir status. For the scheduled day-ahead generation, with the increase in the initial and final reservoir water levels, the generation head increases simultaneously, which means the generation efficiency of the hydropower increases. As shown in the Fig.2, the planned generation in higher initial and final reservoir water levels is usually no less than that in lower initial and final reservoir water levels. This improvement can be significant in certain circumstances. In the 23rd scenario, the planned generation under the initial and final reservoir water level of 417m, 420m, 424m are 5495.92MWh, 7382.64MWh, 7607. 95MWh, respectively. However, with the increase in reservoir water level, the storage capacity decreases at the same time. In some cases, insufficient storage capacity can lead to curtailed water, in return decreasing the planned generation in higher reservoir water level. In 14th scenario, the plan made under the initial and final reservoir water level of 424m gives the worst planned generation of 4563.39 MWh comparing with 4848.92MWh in 417m and 420m.

Fig. 3 shows the reliability of the day-ahead plan in each scenario day under different hydropower reservoir status. With higher reservoir water levels, higher generation plan could be made from the model. This will lead to decrease in reliability of the day-ahead plan. Comparing with the

Table 2
Methods Compared in Case Studies

Method		Description
Control Model	M1	The conventional operation model using the predicted wind power output to make the day-ahead plan directly.
Stochastic Model	M2	Assuming the wind power output forecast error obeys a normal distribution with zero mean as $\sigma_t = 15\% \times N_w^{cap}/2$ considering a confidence level of 95%, and 2000 forecast error representative scenarios are generated through Monte Carlo sampling for each scenario day [17][24].
	M3	Same as M2, but Latin Hypercube Sampling is used [11].
	M4	The adjacent time interval is obtained to depict the fluctuation of wind power prediction, and the upper boundary, wind power output forecast, and lower boundary are taken as the representative scenarios for each scenario day. The method is detailed in [25].
	M5	The proposed method using Decision Tree Regression as the embedded machine learning model.
	M6	Same as M5, but KNN is used.
	M7	Same as M5, but ANN is used.
Tighten-constraint Model	M8	Same as M5, but SVR is used.
	M9	Same as M5, but Random Forest Regression is used.
	M10	Same as M5, but XGBoost is used.
	M11	Same as M5, but LightGBM is used.
	M12	Same as M5, but Gradient Boosting Regression is used.
	M13	Same as M5, but CatBoost is used.

Table 3
Hydropower reservoir status

Reservoir status	Initial and final reservoir water level	Unit
Low reservoir water level, sufficient storage capacity	417	m
Moderate reservoir water level, relative sufficient storage capacity	420	m
High reservoir water level, insufficient storage capacity	424	m

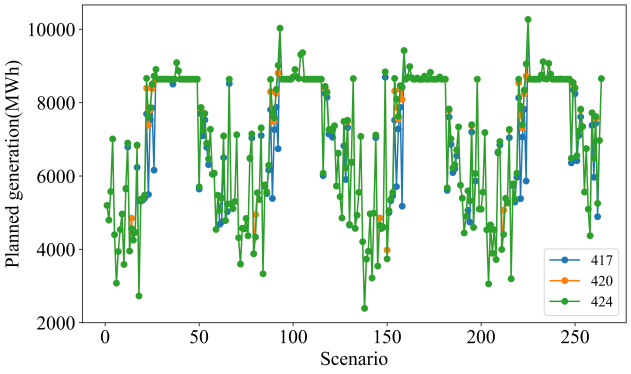

Figure 2: Planned generation under different reservoir status

plans made under the initial and final reservoir water level of 417m, there are 18 scenarios under 420m and 14 scenarios under 424m whose day-ahead plans get lower reliability. However, with higher generation efficiency, the reliability of the day-ahead plan can be improved in some cases. The reliability of the plans under the initial and final reservoir water level of 424m is no less than that in 420m. Even though in some cases, like 25th scenario, the planned generation in 424m is 8504.22MWh which is larger than that under 420m with 8384.06 MWh. Sometimes, when the storage capacity is insufficient, to maintain the smooth output profile, hydropower needs to curtail water and the planned generation decreases which can lead to a higher reliability. As mentioned above, in 14th scenario, the planned generation in 424m is minimum however the reliability is 1 comparing with 0.96 in 417m and 420m.

4.1.3. The effectiveness of M10

Fig.4 represents 3 statistical indices of the results from M1 and M10. The first sub-figure represents the average reliability of unfulfilled scenario days in M1. After using M10, the reliability in the same scenario days increases from around 86% to 99% under different reservoir levels. With the high guarantee in reliability of day-ahead plan, the average standard deviation and average unfulfilled generation over all the test set scenario days drops significantly as shown in the second and third sub-figures.

4.2. Comparison of results for different models

4.2.1. Experiment step

As mentioned in the introduction, when making the day-ahead plan, apart from the conventional model (M1), to handle the inherent uncertainty in wind power forecast,

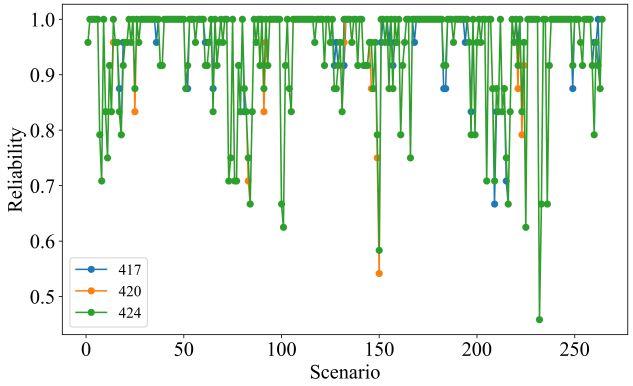

Figure 3: Reliability of day-ahead plan under different reservoir status

typically, stochastic models are used in which the day-ahead plan is essentially the optimum of an statistical average over multiple representative scenarios. To further show the effectiveness of our proposed method, the stochastic models presented in some references are taken for comparison. Meanwhile, different machine learning methods may perform differently when finding the proposed adjustment parameter, in this experiment, a few prominent regression methods are selected for comparison to showcase the influence of the different levels of regression precision on the results as shown in Table 2. According to the results in the previous experiment, when the reservoir water level is low or the storage capacity is insufficient, the results might be influenced. For the following experiments, the initial and final reservoir water levels are set as 420m. For M5-M13, the machine learning models are trained respectively based on the training set. The results are compared under the full testing set.

4.2.2. The reliability and calculation time of day-ahead plan under different models

The reliability of day-ahead plans for the testing set under different models are shown in Fig.5. As shown in the figure, amongst all the models, the M4 performs the worst. It gets the least number of scenario days (48.11% of all scenario days) whose reliability is 1 (reliable plan) and the highest number of scenario days whose reliability is under 0.9. Followed by M1, with only 56.82% of scenario days reach a reliability of 1. Comparing with M1, the M2 and M3 improve the number of scenario days with reliable plan to 81.44% and 76.52%, respectively. The reason why M3 gets a fewer number of reliable plans lies in the differences of random sampling between Monte Carlo and LHS. As LHS uses stratified sampling to consider extreme conditions, it might have a more optimistic expectation for real-time wind power output. This will lead to a higher generation plan while decrease the reliability. Comparing with the highest 81.44% in stochastic model M2, the lowest one reaches 93.94% (M13) and the highest one reaches 99.62% (M5) after using the proposed method. A high reliability plan can always be expected after using our method.

The average converge elapsed time under different models and computation burden comparing with M1 are shown in Table 4. While the M2 and M3 have a relative higher ability than M1 in making a reliable plan, they incur significant computation burden simultaneously. By comparison, a higher reliable plan rate without extra computation burden can be achieved after using our method in M5-M13.

4.2.3. Optimal gap under M5-M13

For the grid operator, high reliability in day-ahead plan can improve the reliability and operational security for the real-time grid operation. However, the less total generation planned in day-ahead plan, the higher reliability might be achieved in real-time operation. In other words, when the generation in day-ahead plan is set as 0, this plan can always get a reliability of 1 in real-time operation. Under the context of electricity markets, how to plan more generation under the premise of high day-ahead plan reliability can benefit both the SO and generator. Therefore, given the guarantee of high reliable plan rates in M5-M13, further discussion should be put on another dimension, i.e. the efficiency in using resources in the WHHPS for generation.

In this context, the optimal generation plan refers to the reliable day-ahead plan with largest generation. The optimal generation plan can be obtained by the introduced tightened-constraint method with the introduced λ calculating from the bilevel game model. The optimal gap refers to the difference between the generation in optimal generation plan (G^{Opt}) and the generation in the reliable day-ahead plan made in each models (G^{Plan}). The cross validation results of the machine learning models in M5-M13 for this experiment are shown in Appendix B.

Ranking the test scenario days by the generation in the optimal generation plan, the relationship between the G^{Opt} and G^{Plan} in the corresponding scenario in M5-M13 is shown in Fig. 6. As shown in the figure, The optimal gap can vary significantly in different models. Although the M5 can make the most reliable plans, the average optimal gap in these plans is 1436.57 MWh, which is much larger than the smallest one of M13 with only 489.64 MWh.

As the only difference between M5-M13 is the different choice of machine learning model, this large optimal gap difference might come from the different ability in predicting the proposed adjustment parameter. Therefore, to show this relationship, the prediction precision of adjustment parameter in these scenario days, whose reliability of the day-ahead plans made in M5-M13 are all 1, are calculated as the R^2 with eq.(12)[43]. The relationship between prediction precision of the proposed adjustment parameter and optimal gap is shown in Fig.7. With the improvement in prediction precision of the adjustment parameter, the marginal benefit increases, which means per unit increase in prediction precision can bring a larger and larger decrease in optimal gap.

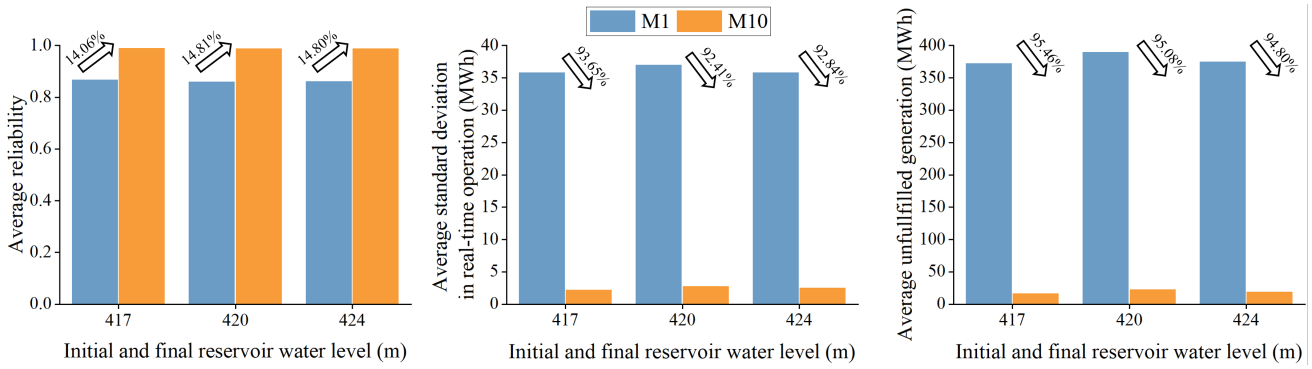

Figure 4: Comparison of M1 and M10 under different reservoir status

Table 4
Converge time

@Models	Converge time(s)	Burden rate	Models	Converge time(s)	Burden rate
@ M1	0.005	\	M8	0.005	0%
@ M2	1.349	26880%	M9	0.005	0%
@ M3	1.42	28300%	M10	0.005	0%
@ M4	0.007	40%	M11	0.005	0%
@ M5	0.005	0%	M12	0.005	0%
@ M6	0.005	0%	M13	0.005	0%
@ M7	0.005	0%	\	\	\

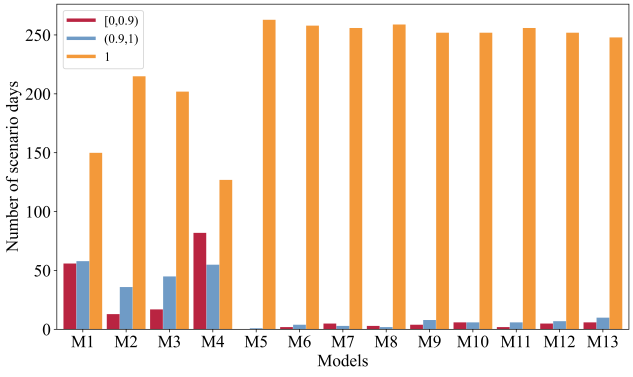

Figure 5: Reliability distribution of testing set under different models

$$R^2_{Mi} = 1 - \frac{\sum_{s=1}^{S}\sum_{t=1}^{T-1}(\lambda_{t,s}^{Mi} - \lambda_{t,s}^{*})^2}{\sum_{s=1}^{S}\sum_{t=1}^{T-1}(\lambda_{t,s}^{*} - \bar{\lambda^{*}})^2}, i = \{5, 6, \cdots, 13\} \tag{12}$$

Where $\lambda_{t,s}^{*}$ is the actual optimal value obtained from the MILP, $\lambda_{t,s}^{Mi}$ is the predicted value and $\bar{\lambda^{*}}$ is the average of all actual value. S is the scenario days set.

4.3. Relationship between training set size and results

4.3.1. Experimental step

As shown in the previous experiments, after using M5-M13, the high reliability of day-ahead plan can be guaranteed and with the increase in prediction precision of the proposed adjustment parameter, the optimal gap can be decreased faster and faster. Previous research has shown the simulating performance of the machine learning methods can be affected by parameter settings[44]. In this paper, rather than trying different hyper parameters to investigate the influence of model parameters on the prediction precision of the proposed adjustment parameter, we hope to explore the relationship between the size of training data set and results. Based on a training set of 1200 scenario days, we started with 48 scenario days and added 48 scenario days each time, resulting in a total of 25 training subsets. According to the previous experiment, the M13 is used in this part. We use each subset to train the CatBoost in M13 and the testing set is used for comparison.

4.3.2. Training set size and reliability

Fig.8 shows the percentage of reliable plan in testing set. Under different training set sizes, this portion remains a high level over 91.29% and reaches a maximum of 97.35%. As before, the R^2 is chosen to show the prediction precision. The relation of the prediction precision of the proposed adjustment parameter over the training set size is shown in Fig.9. The figure suggests a continuous growing trend in

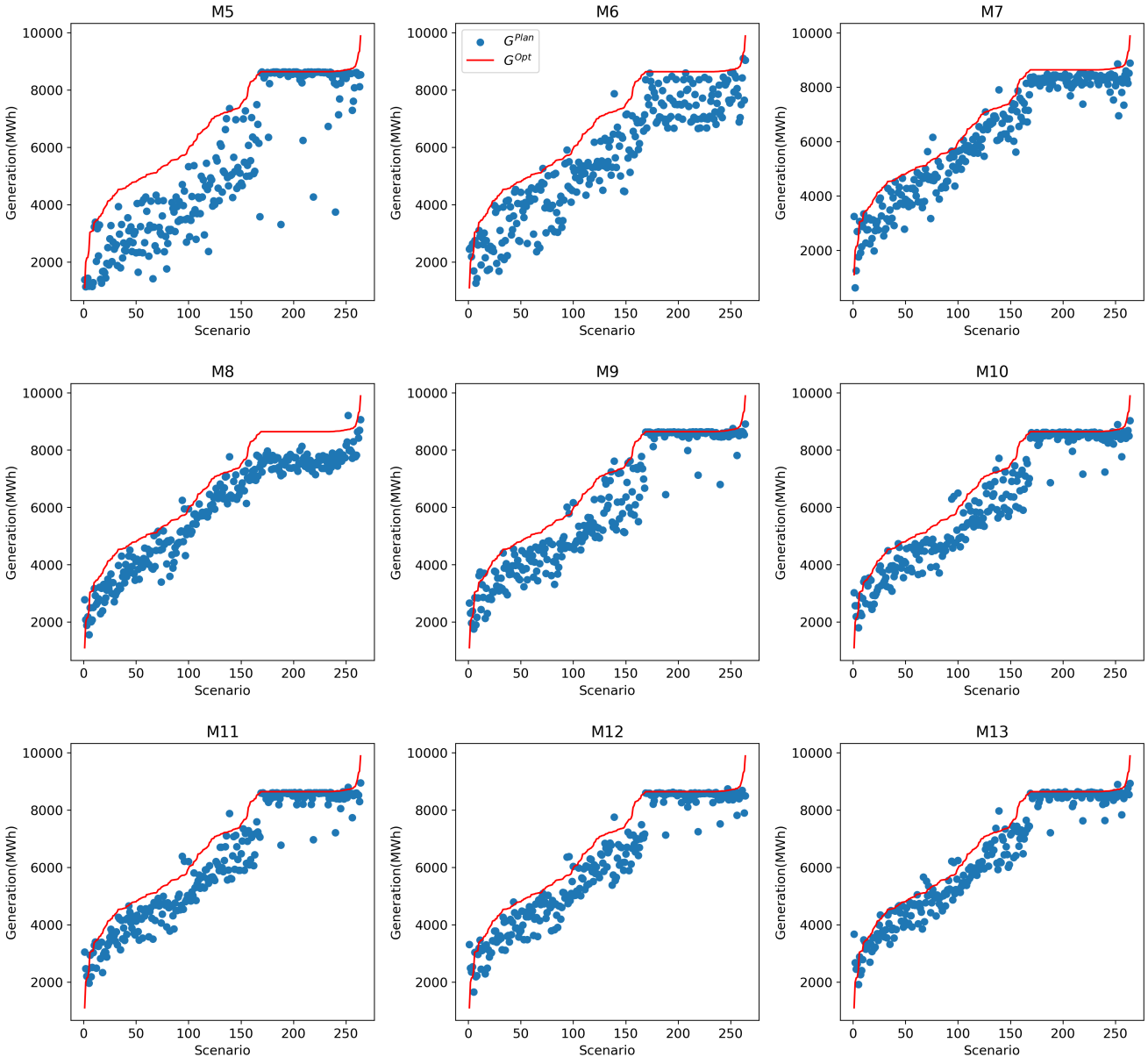

Figure 6: Comparison of the relationship between G^{Opt} and G^{Plan} in M5-M13

prediction precision, however, the marginal gain increases significantly at first and decreases later.

4.3.3. Training set size and optimal gap

Having shown the ability of our method in producing reliable day-ahead plans in previous results, to further show the influence of training set size on optimal gap, 6 scenario days are selected for analysis as shown in Fig.10. In general, with the increase in training set size, a decrease trend in optimal gap can be seen. In some cases, like case 2, the optimal gap drops significantly by 67.6% at first. Similar results can be obtained from case 5, 7, 9. The average optimal gap of the scenario days with reliable plans under different training data set is shown in Table 5. With the increase in training set size, the optimal gap can drop by more than 50%, which can improve the efficiency in resources utilization and guarantee the profit of the WHHPS.

5. Conclusion

From the perspective of real-time operation, this paper proposes a new tighten-constraint method for WHHPS to improve the effectiveness of the day-ahead plan. First, a conventional multi-objective day-ahead planning model for the WHHPS considering generation and output fluctuation is formulated. By using ε-constraint method, the multi-objective model is reformulated as a single objective model. Then, with the help of McCormick convex relaxation and choosing a fluctuation averse strategy, the non-convex single

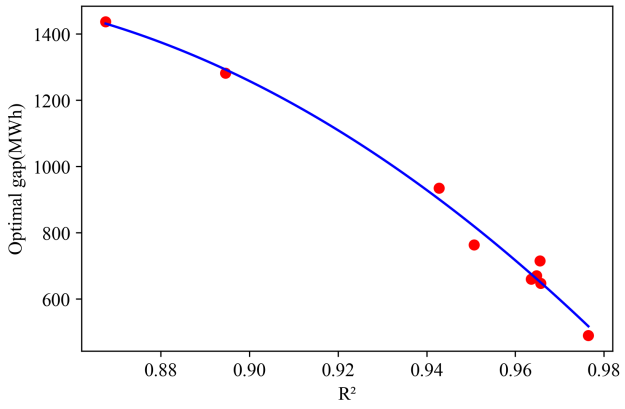

Figure 7: Relationship between optimal gap and prediction precision of the adjustment parameter

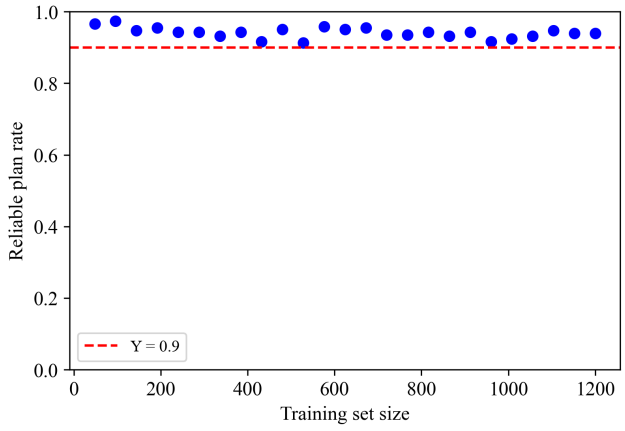

Figure 8: Relationship between training set size and reliable plan rate

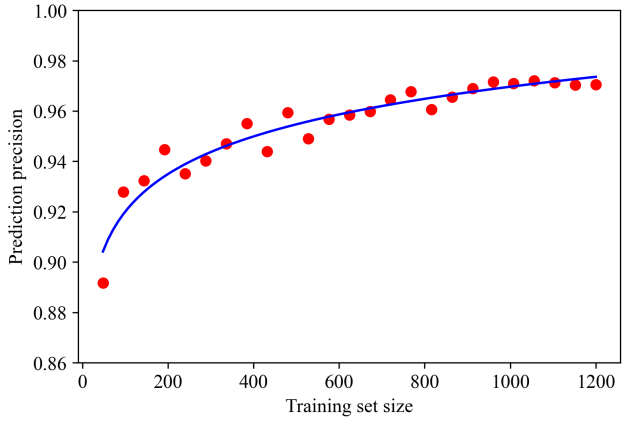

Figure 9: Relationship between training set size and prediction precision

objective model is reformulated as a LP. The fulfillment of day-ahead plan in real-time operation is formulated as a

Table 5
Optimal gap under different training set size(MWh)

Training set size	Optimal gap	Training set size	Optimal gap
48	1194.52	672	617.6192
96	943.7891	720	598.9485
114	817.5091	768	551.3343
192	805.2866	816	613.7816
240	813.7606	864	524.9576
288	792.8734	912	541.6922
336	692.3983	960	512.9952
384	661.7904	1008	512.3668
432	660.3133	1056	491.3405
480	647.3919	1104	508.481
528	625.1581	1152	513.2965
576	681.75	1200	509.9319
624	632.545	\	\

MIP and the reliability metric is proposed to evaluate the day-ahead plan from the perspective of real-time operation. To handle the error in wind power output forecast which may lead to low reliability of the day-ahead plan, a tighten-constraint method by introducing an adjustment parameter is introduced and a bilevel game-theoretic framework is proposed to determine the adjustment parameter. The tighten-constraint day-ahead planning model is considered in the lower level problem, while a reliable and high generation day-ahead plan from the perspective of real-time operation is considered in the upper level problem. Then the bilevel model is transformed into a single-level MILP and the data-driven process is clarified. Numerical results are presented to demonstrate the feasibility and effectiveness of the proposed tighten-constraint method and the influence of prediction precision on the proposed adjustment parameter is discussed. The main conclusions drawn are as follows:

(1) In M1, there is no absolute relationship between the hydropower reservoir status and reliability of the day-ahead plan. However, a sufficient storage and high reservoir water level may improve the reliability. The proposed method can improve the reliability, decrease real-time operation fluctuation and unfulfilled generation in all hydropower reservoir status.

(2) M2 and M3 can improve the reliability of the day-ahead plan but they will lead to computation burden simultaneously (26880% and 28300% burden rate respectively in case study). In contrast, M5-M13 can guarantee a higher level of reliability for the day-ahead plan while at the same time rely on no additional computation burden (0% burden rate). However, the optimal gap of the planned generation under M5-M13 can vary because of different ability in finding the best adjustment parameter. This can be further alleviated by using more training data as the WHHPS continues to operate over long-term.

(3) A high level of completion rate can always be found (larger than 0.91 of reliable plan rate in the case study) even though when the training set size is relatively small. However, with larger training set size, there would be an

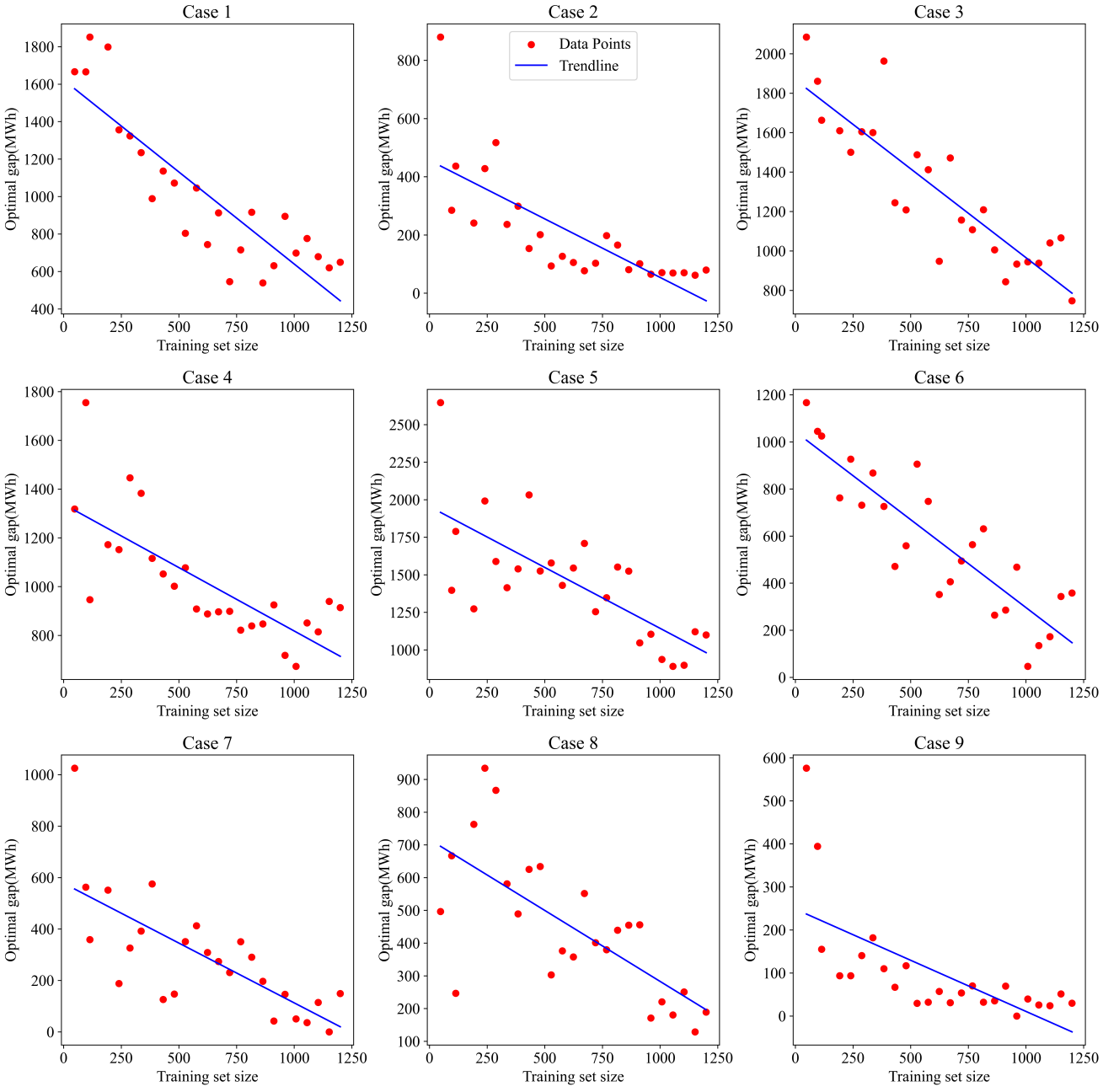

Figure 10: Relationship between training set size and optimal gap

increase trend in prediction precision of the proposed adjustment parameter and decrease trend in optimal gap of the planned generation (from 1194.52 MWh to 509.93 MWh in case study).

In conclusion, the proposed tighten-constraint method gives a new way to guarantee a high reliability for the day-ahead plan from the perspective of real-time operation given wind power output forecast uncertainty for WHHPS, and with the increase of historical data, a plan which has high efficiency in resource utilization for generation can be expected. This method can be applied to the hybrid power system consisting of both variable RES and complementary power source. However, this method only considers the hybrid power system with 1 RES power plant and 1 complementary power plant which limits its application. For the hybrid power systems with more than 1 RES power plant or 1 complementary power plant, further research should be carried out to prove the effectiveness of the proposed method. At the same time, it is worth mentioning that this method is not fully explored. At this stage, we only consider improving the reliability of the day-ahead plan under the circumstance when wind power output forecast is overestimated, which means this method may not guarantee a best resource utilization in real-time operation under all conditions. In addition,

this study only obtains one-year forecast and actual output data from four wind generators and further data collection is needed to enhance the capability of this method in increasing efficiency in resources utilization. The future work can be extended into the context of electricity power marketization to estimate potential profit gains as a result of applying the proposed method to both the generation company and SO. Meanwhile, further works can be carried out to test the performance of the proposed method in systems with high levels of wind power integration and there is potential to extend this research to address challenges in long-term operation horizons.

A. Algorithm for checking the relaxation accuracy

The procedure of relaxation accuracy checking is shown in Algorithm 1. For the WHHPS used in case study, $I = J = 100$.

Algorithm 1 Approximation accuracy check

Initialize the testing data grid $G = \{(Q_{g,i}, h_j)|i = 1, 2, \cdots, I; j = 1, 2, \cdots, J\}$
$TE = 0, n = 0$
for $i = 1$ to I **do**
  for $j = 1$ to J **do**
    $N_h = kQ_{g,i}h_j$
    $L = \max\{Q_g^{min}h_j + h^{min}Q_{g,i} - Q_g^{min}h^{min}, Q_g^{max}h_j + h^{max}Q_{g,i} - Q_g^{max}h^{max}\}$
    $U = \min\{Q_g^{max}h_j + h^{min}Q_{g,i} - Q_g^{max}h^{min}, Q_g^{min}h_j + h^{max}Q_{g,i} - Q_g^{min}h^{max}\}$
    if $N_h \le N_h^{max}$ or $L \le N_h^{max}$ **then**
      $N_h = \min\{N_h, N_h^{max}\}$
      $U = \min\{U, N_h^{max}\}$
      $L = \min\{L, N_h^{max}\}$
      $E = \max\{|N_h - U|, |N_h - L|\}$
      $TE+ = \frac{E}{N_h}$
      $n+ = 1$
    end if
  end for
end for
$A = \frac{TE}{n}$

B. Cross validation results

The cross validation results of the machine learning models in the M5-M13 are shown in Table 6.

CRediT authorship contribution statement

Chunyang Lai: Conceptualization, Methodology, Software, Validation, Writing - original draft. **Behzad Kazemtabrizi:** Conceptualization, Methodology, Supervision, Writing - review & editing.

Declaration of Competing Interest

The authors declare that they have no known competing financial interests or personal relationships that could have appeared to influence the work reported in this paper.

Acknowledgement

This study was supported by the China Scholarship Council.

Data availability

Data will be made available on request.

References

[1] J. Lee, F. Zhao, Global wind report 2021, Global Wind Energy Council 75 (2021).

[2] Y. Wang, R. Zou, F. Liu, L. Zhang, Q. Liu, A review of wind speed and wind power forecasting with deep neural networks 304 117766. doi:10.1016/j.apenergy.2021.117766.
URL https://www.sciencedirect.com/science/article/pii/S0306261921011053

[3] Y. Zhang, C. Cheng, H. Cai, X. Jin, Z. Jia, X. Wu, H. Su, T. Yang, Long-term stochastic model predictive control and efficiency assessment for hydro-wind-solar renewable energy supply system 316 119134. doi:10.1016/j.apenergy.2022.119134.
URL https://www.sciencedirect.com/science/article/pii/S0306261922005128

[4] H. Li, R. Zhang, M. A. Mahmud, B. Hredzak, A novel coordinated optimization strategy for high utilization of renewable energy sources and reduction of coal costs and emissions in hybrid hydro-thermal-wind power systems 320 119019. doi:10.1016/j.apenergy.2022.119019.
URL https://www.sciencedirect.com/science/article/pii/S0306261922004251

[5] Y. Li, T. Zhang, X. Deng, B. Liu, J. Ma, F. Yang, M. Ouyang, Active pressure and flow rate control of alkaline water electrolyzer based on wind power prediction and 100% energy utilization in off-grid wind-hydrogen coupling system 328 120172. doi:10.1016/j.apenergy.2022.120172.
URL https://www.sciencedirect.com/science/article/pii/S0306261922014295

[6] M. Mahdavi, F. Jurado, R. A. V. Ramos, A. Awaafo, Hybrid biomass, solar and wind electricity generation in rural areas of fez-meknes region in morocco considering water consumption of animals and anaerobic digester 343 121253. doi:10.1016/j.apenergy.2023.121253.
URL https://www.sciencedirect.com/science/article/pii/S0306261923006177

[7] S. Zhou, Y. Han, A. S. Zalhaf, S. Chen, T. Zhou, P. Yang, B. Elboshy, A novel multi-objective scheduling model for grid-connected hydro-wind-pv-battery complementary system under extreme weather: A case study of sichuan, china 212 818–833. doi:10.1016/j.renene.2023.05.092.
URL https://www.sciencedirect.com/science/article/pii/S0960148123007243

[8] J. Jiang, B. Ming, Q. Huang, J. Chang, P. Liu, W. Zhang, K. Ren, Hybrid generation of renewables increases the energy system's robustness in a changing climate, Journal of Cleaner Production 324 (2021) 129205.

[9] L. Wen, K. Suomalainen, B. Sharp, M. Yi, M. S. Sheng, Impact of wind-hydro dynamics on electricity price: A seasonal spatial econometric analysis, Energy 238 (2022) 122076.

[10] C.-K. Woo, I. Horowitz, J. Moore, A. Pacheco, The impact of wind generation on the electricity spot-market price level and variance: The texas experience, Energy Policy 39 (7) (2011) 3939–3944.

Table 6
Cross validation of machine learning model in M5-M13

Machine learning models	Mean RMSE	Mean R-squared score
Decision Tree Regression	0.0639	0.9566
KNN	0.0729	0.9439
ANN	0.0554	0.9694
SVR	0.0649	0.9557
Random Forest	0.0435	0.9798
XGBoost	0.0355	0.9866
lightGBM	0.0372	0.9853
Gradient Boosting	0.0376	0.9850
CatBoost	0.0343	0.9890

[11] Y. Guo, B. Ming, Q. Huang, Y. Wang, X. Zheng, W. Zhang, Risk-averse day-ahead generation scheduling of hydro–wind–photovoltaic complementary systems considering the steady requirement of power delivery 309 118467. doi:10.1016/j.apenergy.2021.118467.
URL https://www.sciencedirect.com/science/article/pii/S0306261921016925

[12] C. Peng, Y. Zhang, B. Zhang, D. Song, Y. Lyu, A. Tsoi, A novel ultra-short-term wind power prediction method based on xa mechanism 351 121905. doi:10.1016/j.apenergy.2023.121905.
URL https://www.sciencedirect.com/science/article/pii/S0306261923012692

[13] Y. Li, Z. Wu, Y. Su, Adaptive short-term wind power forecasting with concept drifts 217 119146. doi:10.1016/j.renene.2023.119146.
URL https://www.sciencedirect.com/science/article/pii/S0960148123010601

[14] Y. Zhang, J. Wang, X. Wang, Review on probabilistic forecasting of wind power generation 32 255–270. doi:10.1016/j.rser.2014.01.033.
URL https://linkinghub.elsevier.com/retrieve/pii/S1364032114000446

[15] A. Ajagekar, F. You, Deep reinforcement learning based unit commitment scheduling under load and wind power uncertainty 14 (2) 803–812. doi:10.1109/TSTE.2022.3226106.

[16] Y. Yin, T. Liu, C. He, Day-ahead stochastic coordinated scheduling for thermal-hydro-wind-photovoltaic systems 187 115944. doi:10.1016/j.energy.2019.115944.
URL https://www.sciencedirect.com/science/article/pii/S0360544219316287

[17] M. Xiang, Z. Yang, J. Yu, G. Wang, Determination and cost allocation for regulation reserve with renewables: A data-driven assisted approach 14 (2) 813–825. doi:10.1109/TSTE.2022.3226255.

[18] Z. Zhang, H. Qin, J. Li, Y. Liu, L. Yao, Y. Wang, C. Wang, S. Pei, J. Zhou, Short-term optimal operation of wind-solar-hydro hybrid system considering uncertainties 205 112405. doi:10.1016/j.enconman.2019.112405.
URL https://www.sciencedirect.com/science/article/pii/S0196890419314128

[19] P. P. Biswas, P. Suganthan, B. Qu, G. A. Amaratunga, Multiobjective economic-environmental power dispatch with stochastic wind-solar-small hydro power 150 1039–1057. doi:10.1016/j.energy.2018.03.002.
URL https://linkinghub.elsevier.com/retrieve/pii/S0360544218303943

[20] B. Liu, J. R. Lund, S. Liao, X. Jin, L. Liu, C. Cheng, Optimal power peak shaving using hydropower to complement wind and solar power uncertainty 209 112628. doi:10.1016/j.enconman.2020.112628.
URL https://www.sciencedirect.com/science/article/pii/S0196890420301667

[21] L. Wen, B. Sharp, E. Sbai, Spatial effects of wind generation and its implication for wind farm investment decisions in new zealand, The Energy Journal 41 (2) (2020) 47–72.

[22] Z. Li, P. Yang, Y. Guo, G. Lu, Medium-term multi-stage distributionally robust scheduling of hydro–wind–solar complementary systems in electricity markets considering multiple time-scale uncertainties 347 121371. doi:10.1016/j.apenergy.2023.121371.
URL https://www.sciencedirect.com/science/article/pii/S0306261923007353

[23] J. J. Chen, Y. B. Zhuang, Y. Z. Li, P. Wang, Y. L. Zhao, C. S. Zhang, Risk-aware short term hydro-wind-thermal scheduling using a probability interval optimization model 189 534–554. doi:10.1016/j.apenergy.2016.12.031.
URL https://www.sciencedirect.com/science/article/pii/S0306261916317949

[24] L. Yang, Z. Li, Y. Xu, J. Zhou, H. Sun, Frequency constrained scheduling under multiple uncertainties via data-driven distributionally robust chance-constrained approach, IEEE Transactions on Sustainable Energy 14 (2) (2023) 763–776. doi:10.1109/TSTE.2022.3225136.

[25] Y. Yang, J. Zhou, G. Liu, L. Mo, Y. Wang, B. Jia, F. He, Multi-plan formulation of hydropower generation considering uncertainty of wind power 260 114239. doi:10.1016/j.apenergy.2019.114239.
URL https://www.sciencedirect.com/science/article/pii/S0306261919319269

[26] H. Wei, Z. Hongxuan, D. Yu, W. Yiting, D. Ling, X. Ming, Short-term optimal operation of hydro-wind-solar hybrid system with improved generative adversarial networks 250 389–403. doi:10.1016/j.apenergy.2019.04.090.
URL https://www.sciencedirect.com/science/article/pii/S0306261919307500

[27] Y. Dong, H. Zhang, P. Ma, C. Wang, X. Zhou, A hybrid robust-interval optimization approach for integrated energy systems planning under uncertainties 274 127267. doi:10.1016/j.energy.2023.127267.
URL https://www.sciencedirect.com/science/article/pii/S0360544223006618

[28] K. Huang, P. Liu, B. Ming, J.-S. Kim, Y. Gong, Economic operation of a wind-solar-hydro complementary system considering risks of output shortage, power curtailment and spilled water 290 116805. doi:10.1016/j.apenergy.2021.116805.
URL https://www.sciencedirect.com/science/article/pii/S0306261921003081

[29] B. Ming, P. Liu, L. Cheng, Y. Zhou, X. Wang, Optimal daily generation scheduling of large hydro–photovoltaic hybrid power plants 171 528–540. doi:10.1016/j.enconman.2018.06.001.
URL https://www.sciencedirect.com/science/article/pii/S0196890418306101

[30] X. Yang, X. Wang, Z. Leng, Y. Deng, F. Deng, Z. Zhang, L. Yang, X. Liu, An optimized scheduling strategy combining robust optimization and rolling optimization to solve the uncertainty of res-cchp mg 211 307–325. doi:10.1016/j.renene.2023.04.103.
URL https://www.sciencedirect.com/science/article/pii/S0960148123005694

[31] Q. Tan, X. Wen, Y. Sun, X. Lei, Z. Wang, G. Qin, Evaluation of the risk and benefit of the complementary operation of the large wind-photovoltaic-hydropower system considering forecast uncertainty 285 116442. doi:10.1016/j.apenergy.2021.116442.
URL https://www.sciencedirect.com/science/article/pii/S0306261921000106

[32] B. Liu, T. Liu, S. Liao, J. Lu, C. Cheng, Short-term coordinated hybrid hydro-wind-solar optimal scheduling model considering multistage section restrictions 217 119160. doi:10.1016/j.renene.2023.119160.
URL https://www.sciencedirect.com/science/article/pii/S0960148123010753

[33] Y. Zhu, J. Jian, J. Wu, L. Yang, Global optimization of non-convex hydro-thermal coordination based on semidefinite programming 28 (4) 3720–3728. doi:10.1109/TPWRS.2013.2259642.

[34] Y. Yang, S. Chen, Y. Zhou, G. Ma, W. Huang, Y. Zhu, Method for quantitatively assessing the impact of an inter-basin water transfer project on ecological environment-power generation in a water supply region 618 129250. doi:10.1016/j.jhydrol.2023.129250.
URL https://www.sciencedirect.com/science/article/pii/S0022169423001920

[35] S. Boyd, S. P. Boyd, L. Vandenberghe, Convex optimization, Cambridge university press, 2004.

[36] Y. Huang, Q. Wang, J. Xu, A stackelberg-based biomass power trading game framework in hybrid-wind/solar/biomass system: From technological, economic, environmental and social perspectives 403 136806. doi:10.1016/j.jclepro.2023.136806.
URL https://www.sciencedirect.com/science/article/pii/S0959652623009642

[37] B. H. Brito, E. C. Finardi, F. Y. K. Takigawa, Mixed-integer nonseparable piecewise linear models for the hydropower production function in the unit commitment problem 182 106234. doi:10.1016/j.epsr.2020.106234.
URL https://www.sciencedirect.com/science/article/pii/S0378779620300419

[38] G. P. McCormick, Computability of global solutions to factorable nonconvex programs: Part i—convex underestimating problems, Mathematical programming 10 (1) (1976) 147–175.

[39] H. Von Stackelberg, Market structure and equilibrium, Springer Science & Business Media, 2010.

[40] Q. Hong, F. Meng, J. Liu, R. Bo, A bilevel game-theoretic decision-making framework for strategic retailers in both local and wholesale electricity markets 330 120311. doi:10.1016/j.apenergy.2022.120311.
URL https://linkinghub.elsevier.com/retrieve/pii/S0306261922015689

[41] J. Fortuny-Amat, B. McCarl, A representation and economic interpretation of a two-level programming problem, Journal of the operational Research Society 32 (1981) 783–792.

[42] Rts-gmlc.
URL https://github.com/GridMod/RTS-GMLC

[43] D. Zhang, B. Chen, H. Zhu, H. H. Goh, Y. Dong, T. Wu, Short-term wind power prediction based on two-layer decomposition and bitcn-bilstm-attention model 285 128762. doi:10.1016/j.energy.2023.128762.
URL https://www.sciencedirect.com/science/article/pii/S0360544223021564

[44] Z.-k. Feng, W.-j. Niu, T.-h. Zhang, W.-c. Wang, T. Yang, Deriving hydropower reservoir operation policy using data-driven artificial intelligence model based on pattern recognition and metaheuristic optimizer 624 129916. doi:10.1016/j.jhydrol.2023.129916.
URL https://www.sciencedirect.com/science/article/pii/S0022169423008582